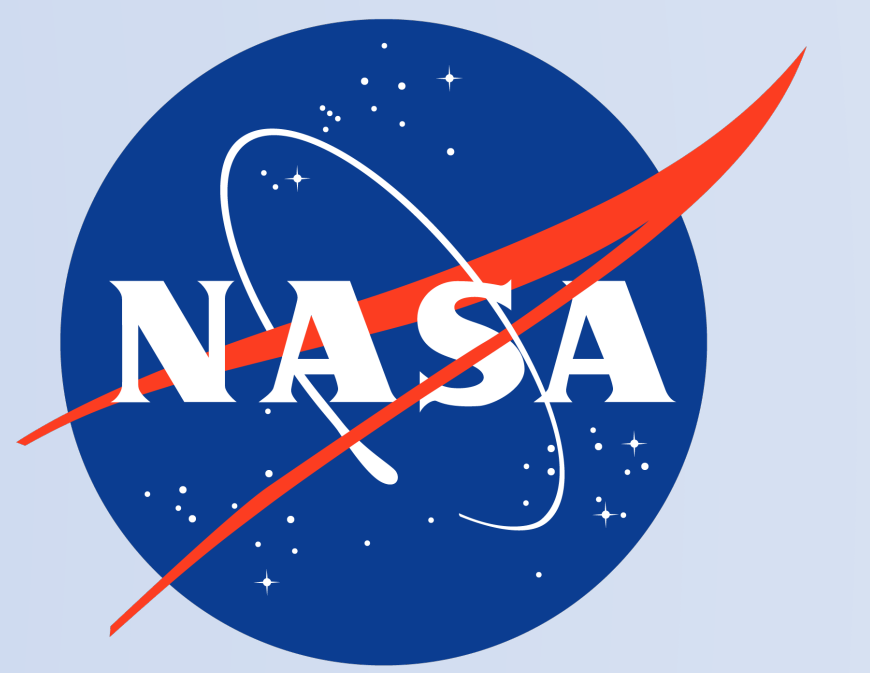


Toward Supersonic Parachute Inflation Capabilities within the Launch, Ascent, and Vehicle Aerodynamics (LAVA) Framework



Jonathan Boustani, Gaetan K. Kenway, Francois Cadieux, Michael F. Barad, Cetin C. Kiris
Computational Aerosciences Branch, NASA Ames Research Center, Moffett Field, CA 94035

18th International Planetary Probe Workshop

Motivation

When the Mars Science Laboratory (MSL) sought to land the heaviest payload at the highest landing site elevation with the highest level of accuracy yet required, a large effort involving many experiments, wind tunnel tests, and drop tests were conducted, none of which were conducted at supersonic speeds. The record in the literature shows computational methods playing exploratory and at most, supporting roles, often with static and rigid geometries of an inflated parachute canopy.

The last few years have seen the maturation of computational methods that are starting to become capable of modeling the complex and nonlinear interaction between an inflating parachute canopy and the supersonic flow in the wake of an entry vehicle in representative flight conditions. The Launch, Ascent, and Vehicle Aerodynamics (LAVA) team is developing efficient, higher-order numerical methods to this end. A loose coupling approach is used to advance the solutions of modularized computational fluid dynamics (CFD) and computational structural dynamics (CSD) solvers in time[1].

Methods

Block-Structured Cartesian AMR Solver

The compressible Navier-Stokes equations are discretized in space on a block-structured Cartesian grid with adaptive mesh refinement (AMR). The use of a block-structured Cartesian grid facilitates the construction of higher-order conservative finite difference shock-capturing schemes. Lagrangian geometries are sharply represented in the Eulerian mesh by a ghost cell immersed boundary method, or ghost cell method (GCM)[2]. Explicit time integration is performed with the classic fourth-order Runge-Kutta (RK) scheme. For second-order accurate interface operators, only one layer of grid points 'inside' of a water-tight representation of the geometry need to be filled, these are so-called ghost cells. For treating thin geometries (with a thickness at or below the local volume grid spacing), however, a ghost-in-fluid approach is used to define ghost cells outside of the geometry representation while maintaining a sharp representation of the immersed boundary[3].

Structural Finite Element Solver

The balance of linear momentum describing the equilibrium of inertial, internal, and external forces is discretized in space by the finite element method using the total Lagrangian formulation. Closure is provided by the Saint-Venant Kirchhoff constitutive relationship. Stress-strain relationships are derived from the 6DOF MITC3 triangular shell and Timoshenko beam elements that are employed. Shear locking is alleviated in the shell and beam elements using the mixed interpolation of tensorial components (MITC) scheme and reduced integration, respectively. Time integration is performed with the second-order explicit central difference scheme. The structural time step is limited by the stability limit which is recomputed throughout a simulation.

Results

1) Computational Performance

The CFD solver maintains an efficient, hybrid OpenMP-MPI parallelization strategy. The CSD solver was recently extended to have this capability, and its computational performance is evaluated here on a 2.5M DOF problem. 90% parallel efficiency is observed at the highest core count with the hybrid parallelization strategy and overlapped computation and communication.

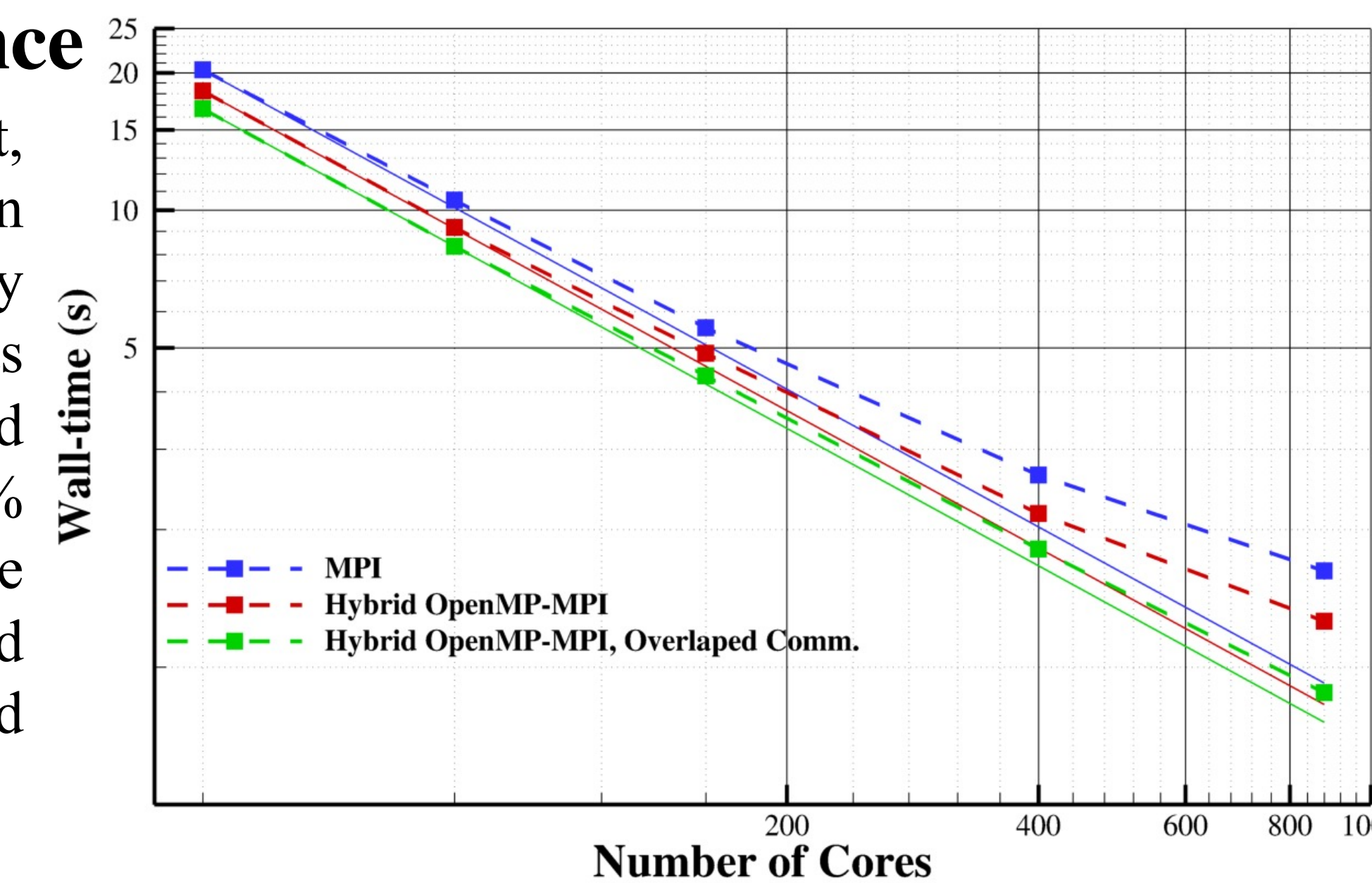


Figure 1: Strong scaling study of the LAVA-Structural solver.

3) Porous Broadcloth Modeling

A model for flow through permeable broadcloth was implemented into the CFD solver. Because of the very small thickness of PIA-C-7020D broadcloth ($O(10\mu m)$), the porous wall is implemented as an interface/jump condition as opposed to typical source term forcing. This model is derived from the high Reynolds number correction to Darcy's law, the Darcy-Forchheimer momentum equation, and the material and inertial permeability coefficients are determined empirically from experimental data[4].

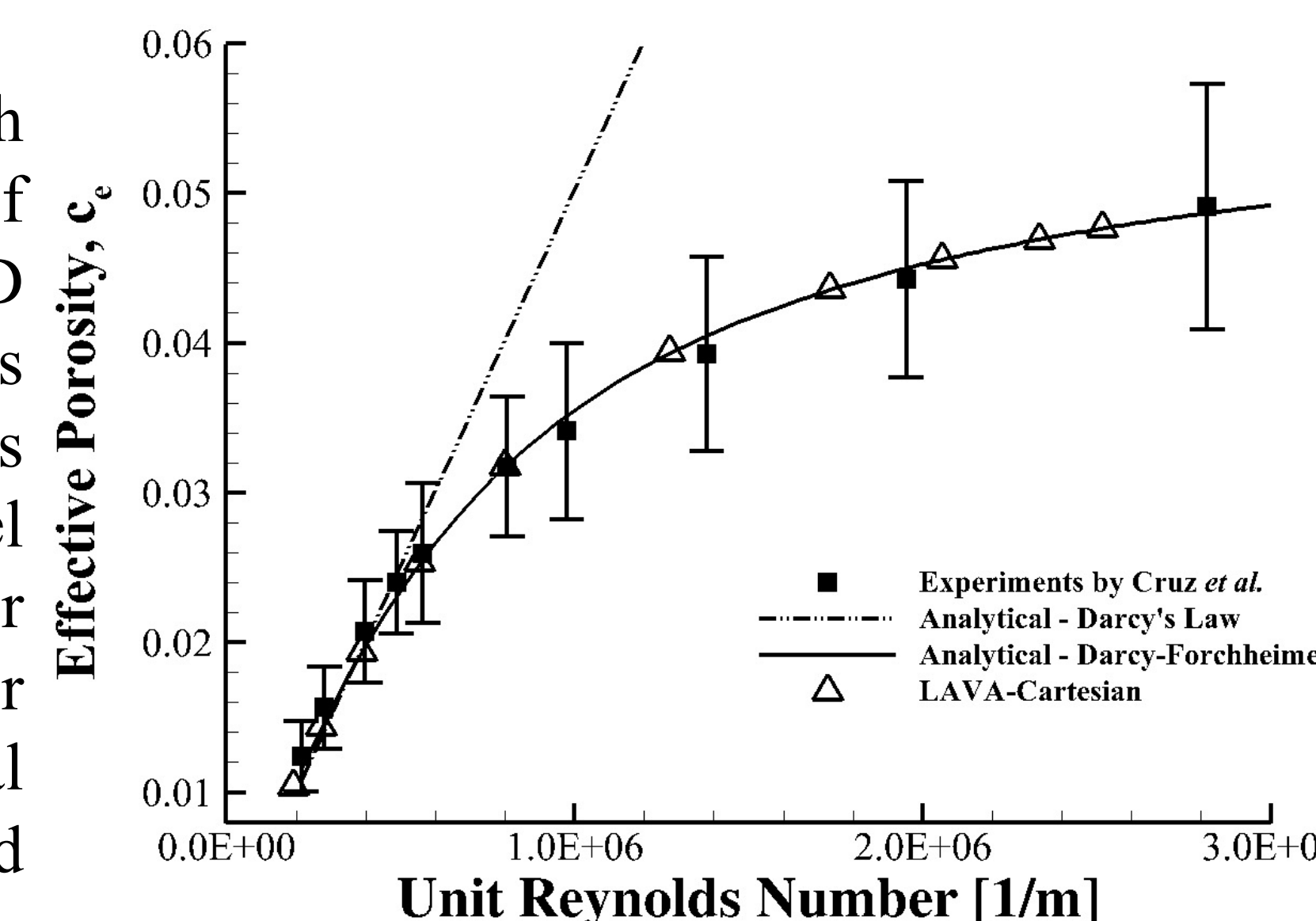


Figure 3: Comparison of numerical, analytical, and experimental results for flow through PIA-C-7020D.

4) Supersonic Parachute Flight

In preparation for full-scale fluid-structure interaction simulations of the ASPIRE SR01 supersonic parachute, the developments made so far are evaluated on a sub-scale, 0.813m nominal diameter DGB parachute in supersonic uniform flow ($M=2.2$). In this study, the aerodynamic performance of an impermeable parachute canopy is compared against canopies modeled by PIA-C-44378D (less porous) and PIA-C-7020D (more porous) broadcloth using the developed porosity model.

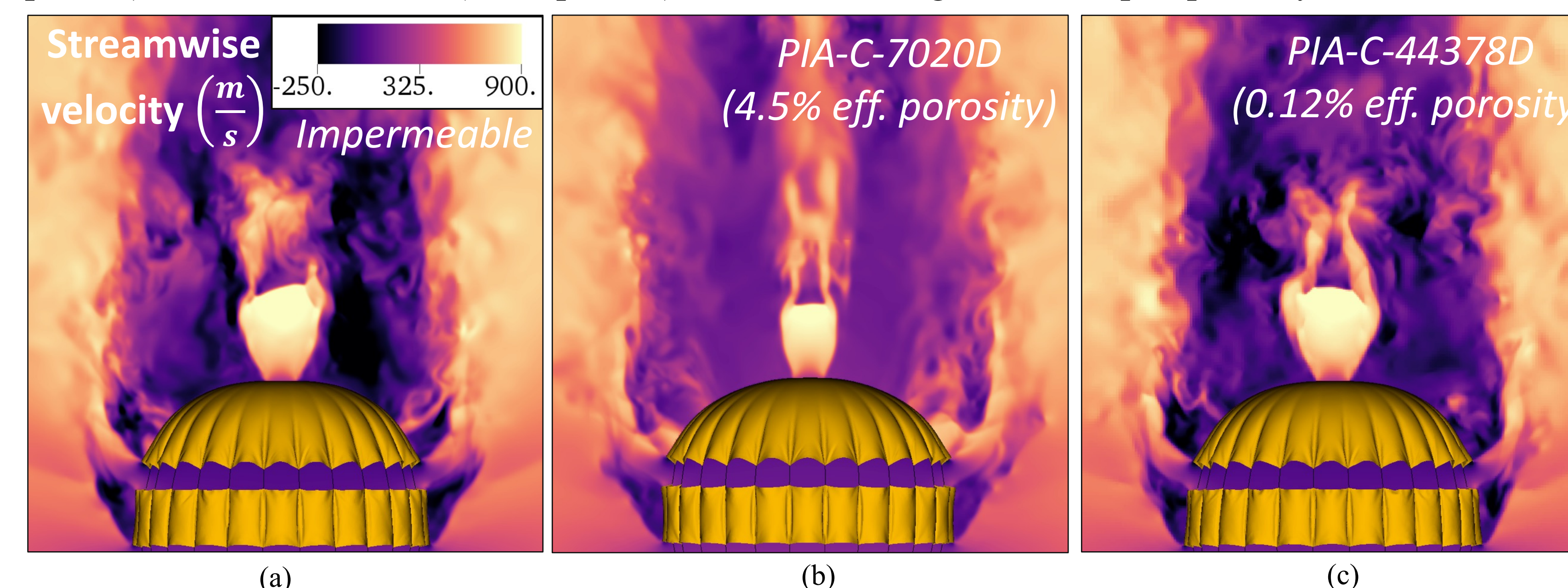


Figure 4: Comparison of the streamwise velocity field for (a) impermeable, (b) PIA-C-7020D, and (c) PIA-C-44378D parachute canopies. The significant increase in porosity on the PIA-C-7020D canopy results in a weaker recirculation region in the wake. This may imply more stable flight due to the decreased interaction between the recirculation region and the parachute canopy. At this Mach number and unit Reynolds number, the PIA-C-44378D has a very low porosity and performances similarly to the impermeable canopy.

2) Contact Mechanics

A novel and efficient contact identification and enforcement method was developed to handle the massive (self-)contact that is experienced during the early stages of inflation. In this method, contact between discrete elements comprising the parachute is modeled as an (in)elastic collision. A penalty impulse is then generated by the change in momentum of the contacting elements.

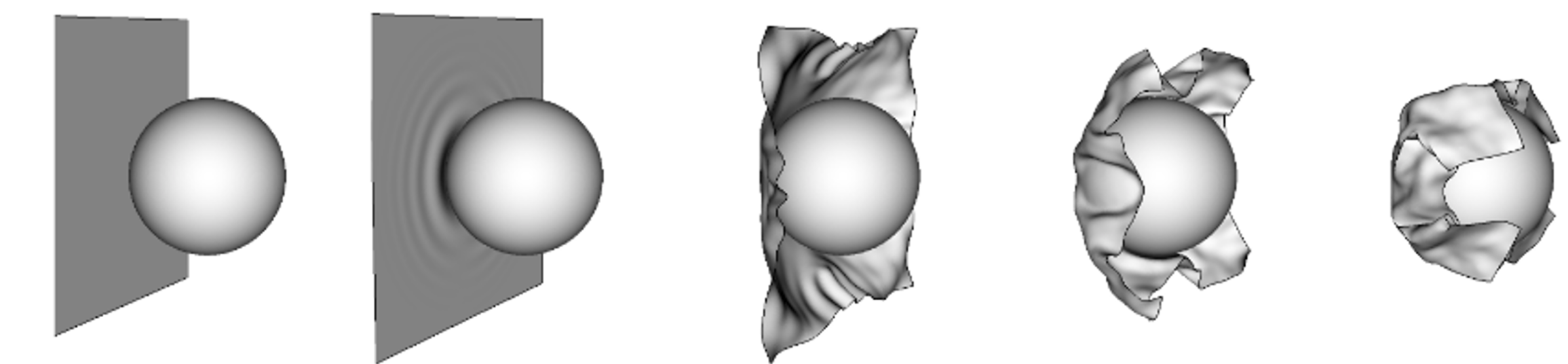


Figure 2: Demonstration of the LAVA-Structural solver on a highly nonlinear contact/impact problem with soft goods.

Conclusions

This poster detailed research that is being conducted within the LAVA framework to support the Entry Systems Modeling project's goal of simulating supersonic parachute inflation. Future tasks include simulating the ASPIRE SR01 supersonic parachute and comparing the aerodynamic performance with experimental data.

Acknowledgements

This research is partially supported by NASA's Entry Systems Modeling (ESM) project and NASA's Transformational Tools and Technologies (T³) project. Computational resources were provided by NASA Advanced Supercomputing (NAS) at NASA Ames Research Center.

References

- [1] Boustani, Jonathan, et al. "An immersed boundary fluid-structure interaction method for thin, highly compliant shell structures." *Journal of Computational Physics* 438 (2021): 110369.
- [2] Mittal, Rajat, et al. "A versatile sharp interface immersed boundary method for incompressible flows with complex boundaries." *Journal of computational physics* 227.10 (2008): 4825-4852.
- [3] Nakahashi, Kazuhiro. "Immersed boundary method for compressible Euler equations in the building-cube method." *20th aiaa computational fluid dynamics conference*. 2011.
- [4] Cruz, Juan R., et al. "Permeability of Two Parachute Fabrics-Measurements, Modeling, and Application." *24th AIAA Aerodynamic Decelerator Systems Technology Conference*. 2017.

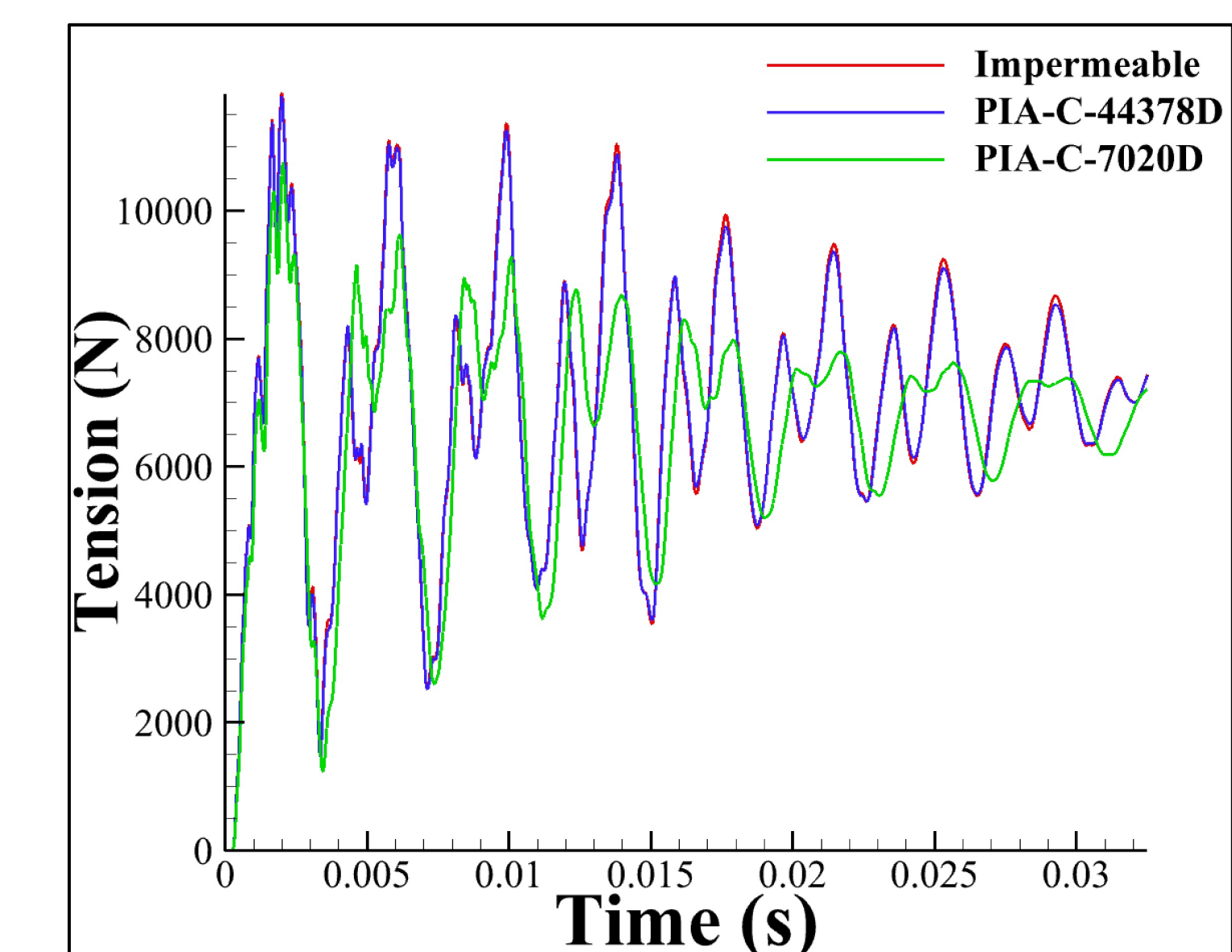


Figure 5: Comparison of the computed tension in the suspension lines for three different parachute canopies in $M=2.2$ flow. The average force is reduced by $\sim 7\%$ between the impermeable and PIA-C-7020D canopies. Thus, there is a tradeoff between aerodynamic drag performance and stability (it is commonly known that more porosity = more stability, until $\sim 80\%$ porosity).